The Title

Frame-based Pinless Stereotaxy.

The Author

Dr. Abdin Khair-Allah Kasim, MD Neurosurgery, Sohag University Hospital, Egypt.

The Short Title

Pinless Stereotaxy.

The Full address:

Postal Address:

Neurosurgery Department, Sohag Faculty of Medicine, Sohag, Egypt.

Postal code:

82511

Phone:

002 093 4591142

Mobile:

002 01020196831

Fax:

002/093/4602963

Email: abdin_neurosurgery@hotmail.com , abdin_mail@yahoo.com

Keywords: Naviplan, Frameless, Pinless, Stereotaxy, Image-guided neurosurgery, Computer–assisted surgery.

Abstract

Background: Frame-based stereotaxy aims at accurate intracranial targeting through fixing a frame to the skull with rigid pins and referring the intracranial targets to this frame followed by frame directed surgery. Pin fixation is a painful step in the operation and, in some situations like in young children having resilient or small skulls and in patients having unsuitable skull defects or previous craniotomies, it may be difficult to be done. Frameless stereotaxy, on the other hand, is not available in many centers.

Objective: To evaluate our new technique of frame-based stereotactic surgery without pin fixation to the skull using a personal software calculator, Naviplan.

Methods:hree small radio-opaque spherical marks are attached to the skull and the intracranial target is referred to a cartesian coordinate system based on them. Intra-operatively, the marks are registered to the frame and the target references are transferred from the mark-based to the frame-based cartesian coordinate system using a personally designed database file (Naviplan).
Results:31 patients were subjected to this method. In all patients, either intra-operative evidence or postoperative radiology was used for accuracy confirmation.
In 15 cases, the aspiration of intracranial cysts and the postoperative CT scans confirmed the accuracy of the procedure. In 16 cases with solid lesions, postoperative CT scan as well as the histopathology yield showed the lesions to be targeted with acceptable accuracy.
Conclusion: Pinless frame-based stereotaxy with Naviplan is easy, save and accurate and can be useful in situations where rigid pins can't be applied.

Full Text

In the era of frameless stereotaxy and emerging intra-operative imaging technologies, stereotactic frames still have their place. They are necessary for the performance of functional surgery, including placement of deep brain stimulators. Brain biopsies arguably are done with the most accuracy and least time using a frame. Stereotactic radiosurgery is always done with a frame except in the unique case of the CyberKnife [1]. Neuronavigation systems, in addition to being expensive and not available in many centers, aim at referring the explored targets rather than directing the surgeon to deep targets through planned trajectories.

Frame based stereotaxy, Radionics CRW system, (Integra Burlington MA, Inc. formerly Integra Radionics, Inc. Burlington, MA [6]) is available in our hospital since the year of 2000 but neuronavigation systems are not available till now. The idea of frame fixation in stereotaxy is to join the cranium and the frame into one unit and refer the target to the frame cartesian coordinate system to approach it based on the frame. Pin fixation constitutes the most painful step throughout the operation and, in some situations like in young children having resilient or small skulls and in patients having unsuitable skull defects or previous craniotomies, it may be difficult to be done. In other patients frame fixation may cause difficulty in endo-tracheal intubation. Pin fixation is not possible in infants. There is risk of cranial fracture, epidural hematoma, and CSF leakage following the application of head pins, especially in young children [2, 3].

Objective: The aim is to evaluate our new technique of stereotactic surgery using the stereotactic frame system without pin fixation to the skull with the help of a new software, Naviplan.

Patients and Methods: After informed written consent, all patients with deep intracranial lesions of at least 2 ml volume who were admitted to our department for biopsy or aspiration since April 2012 till March 2017 were included. Patients who had bleeding tendencies and those who were unfit for surgery were excluded. The following steps were done in all patients.

Patient preparation

Routine investigations to role out bleeding tendency and confirm surgical fitness were carried out and the patient is informed about the steps of the procedure and is requested to fast at least 6 hours before the procedure. Head shaving in males can be done before the procedure.

Mark application

We attach three small radio-opaque spheres to the head. The spheres are 3 mm equal in diameter and tunneled. They were fixed to the head with recoil strings (figure 1).

Figure 1: Spheres position. We joined them with recoil strings and attached two of them in front of both auricles while the 3rd sphere is attached over the root of the nose above the glabella. The spheres positions are marked with a pen marker to notice any displacement during the procedure.

The stability of the scalp marks is an important issue for the procedure accuracy and was addressed as follows:

- The possibility of the spheres to move during the procedure is taken in consideration. For this reason, two of them were attached in front of both auricles where the scalp is least liable to glide over the skull. The glabellar crease is a relatively fixed skull mark anteriorly and the 3rd sphere is attached over the root of the nose above the glabella. All the sphere positions are marked on the scalp with a pen marker to notice any displacement during the whole procedure.
- We added a calculation test layout in the Naviplan file to detect any significant displacement of the spheres.

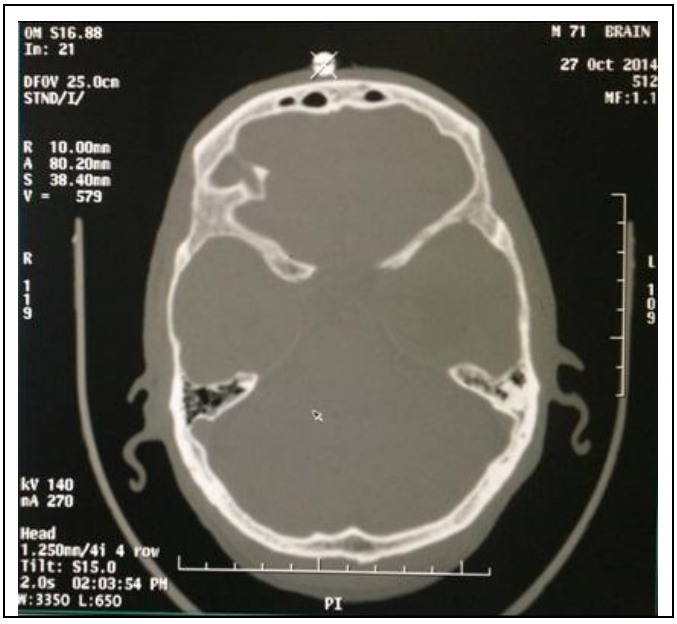

Figure 2: CT Brain. The sphere's center is readily detectable as shown with its CT co-ordinates.

CT scanning

GE 16 slice CT scanner was used in all patients. Thin cuts (1.25 mm) were taken. During the CT scanning, we always check that the patient was not moving and the spheres were in place. In 2 cases we gave IV sedation for the patients because of uncontrolled irritability during the CT scanning. All the other patients were subjected to the CT scanning without sedation. The tunnels of the spheres help to determine the best CT images passing through their centers (Figure 2). The radiological coordinates (X, Y and Z values) for all the mark centers and the targets should be in the same scan series.

Figure 3: Head position. The patient head is positioned inside the stereotactic frame resting on two head posts without any pins.

Anesthesia and positioning

After general anesthesia, the stereotactic frame is fixed to the operating table through the Mayfield adaptor and the patient head is positioned inside the frame resting on two head posts without any pins. We use the longer posts for better head support (Figure 3). Antibiotics are given prior to the incision, sterilization proceeds and a suitable skull burr hole is freely chosen according to the target location.

Registration to the Frame

After the burr hole is made we attach the stereotactic arc base to the frame and start to measure the stereotactic co-ordinates of the three sphere centers manually in relation to the arc. For this purpose, we managed to measure the position of each mark in relation to the frame base with the help of a kirschner wire. The spherical marks have the same radius of 3 mm to help accurate measurement. It is important for the frame to be caudal enough to the scalp marks when the head is positioned for easy measurement (Figure 4).

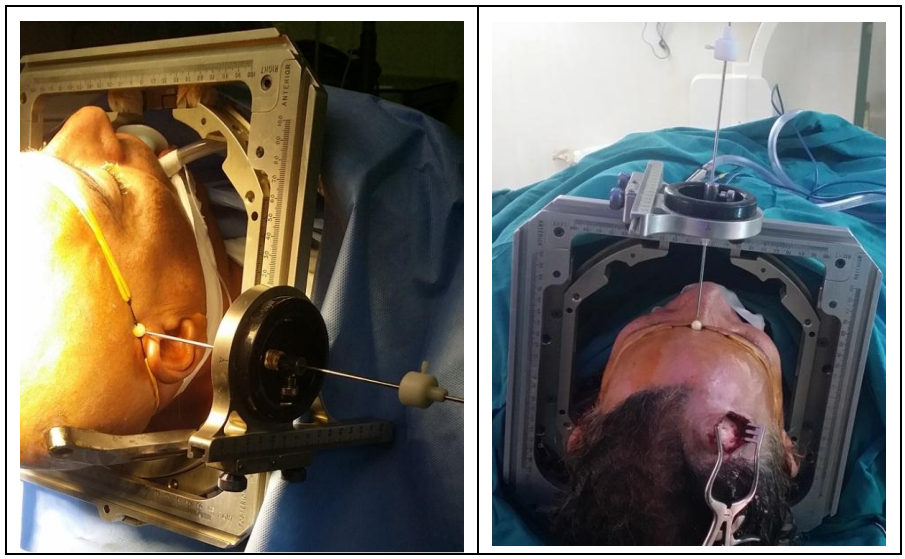

Figure 4: Manual registration of spheres to the stereotactic frame. After the burr hole is made we attach the stereotactic arc base and start to measure the stereotactic co-ordinates of the three spheres manually in relation to the arc.

This step is similar to registration step in neuro-navigation. We delay the registration after doing the burr hole and after insurance of deep anesthesia so that the skull will not move from its final position after that. For easier way, we always considered the center of the right sphere as point 1, the center of the left sphere as point 2 and the center of the forehead sphere as point 3.

Calculation of stereotactic target co-ordinates

At that stage we have two sets of co-ordinates for the three spherical marks; radiologically derived set of X, Y and Z values and stereotactic set of co-ordinates manually measured in relation to the frame. Now we input these two sets of co-ordinates to the Naviplan file (Figure 5) and, on feeding the target radiologically derived X, Y and Z values, it directly calculates the stereotactic co-ordinates of the target (Figure 6). Naviplan is a personal database file designed specifically to calculate the target co-ordinates.

Naviplan file calculation accuracy was tested in the following way:

- The output values for 73 targets in cases previously calculated by Egyplan file were compared to those calculated by Naviplan file providing the same previous radiological and stereotactic co-ordinates of points 2, 5 and 8 (the height points) of the Radionics localizer instead of the 3 sphere centers (Table 1).

- The spheres were attached in 3 previous patients in conjunction to the stereotactic frame during ordinary stereotactic procedures and in each case the target co-ordinates were calculated in two ways, the

first way using the stereotactic localizer and Egyplan file calculations and the second way using the three spheres and Naviplan file calculations.

- In the first 3 patients of the current study, we attached a 4th sphere to the scalp as a test target for evaluation of the accuracy of the procedure (Figure 7).

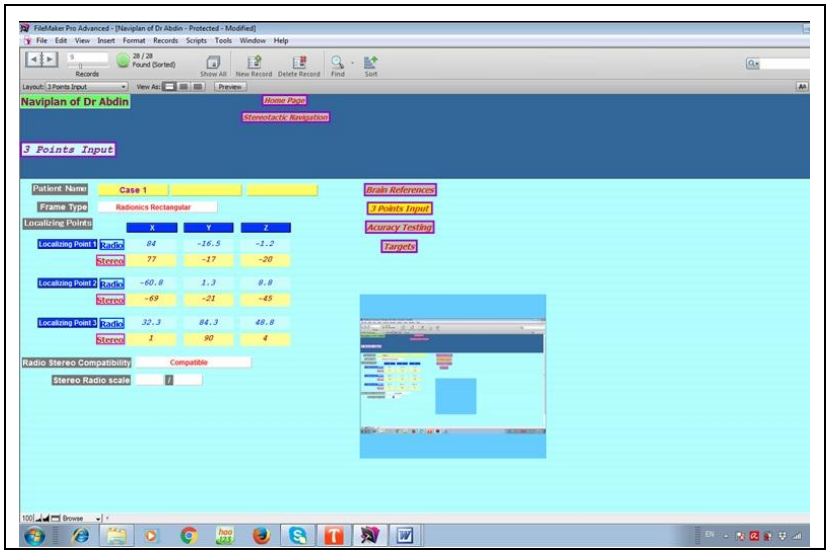

Figure 5: Data Input. In the Naviplan file, we input the two sets of co-ordinates of the three spheres to the Naviplan file. The first data set is radiologically-derived and The second data set is stereotaxy-derived.

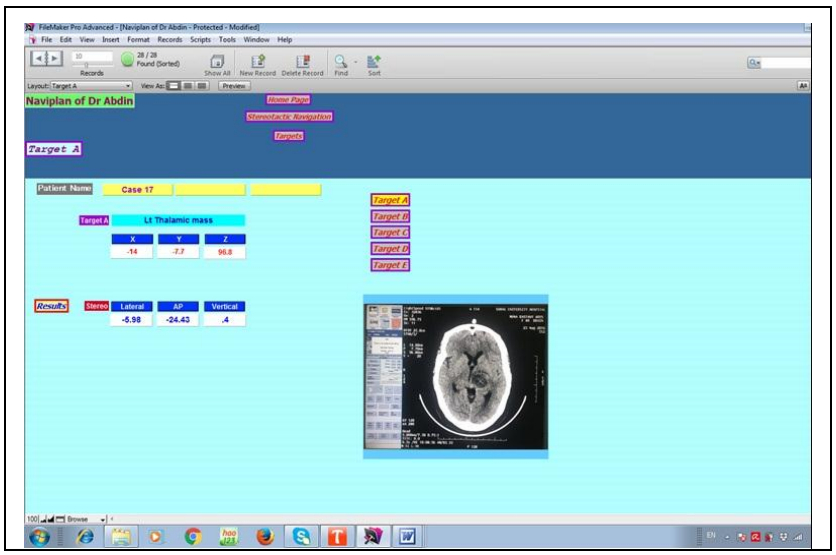

Figure 6: Stereotactic Target Co-ordinates. On feeding the Naviplan file with the target X, Y and Z radiological values, it directly calculates the stereotactic co-ordinates of the target.

Figure 7: Test target. In the first 3 patients we attached a 4th sphere to the scalp as a test target for evaluation of the accuracy of the procedure.

Tissue biopsy

The final steps are done after adjusting the arc system to the target co-ordinates and manipulating the ring and arc angles so that the biopsy needle lines up with the burr hole in its way to the target (Figure 8). After obtaining the biopsy or aspirate, the arc system is removed and the wound is closed and dressed.

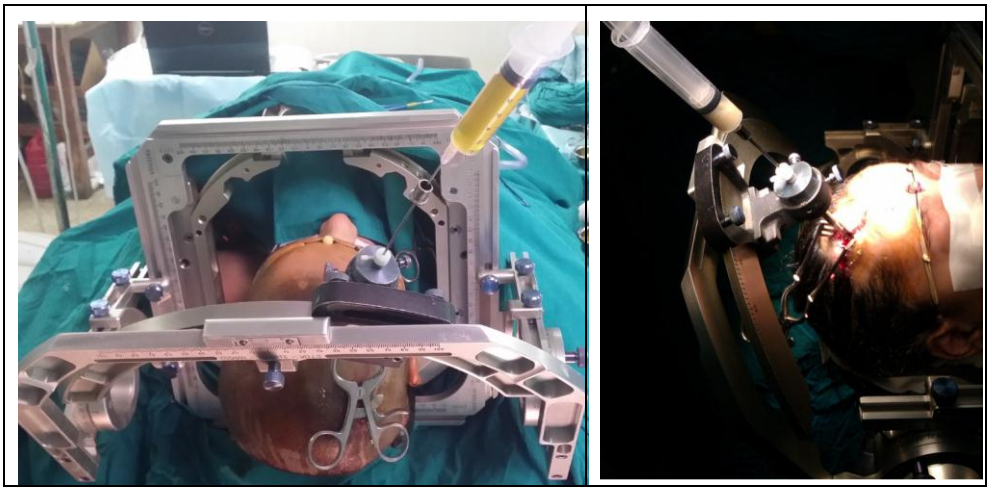

Figure 8: Biopsy. Near complete aspiration of a brain stem cystic lesion radiologically estimated to be about 12 cm3 in volume (left) and complete aspiration of a left thalamic cystic lesion radiologically estimated to be about 4 cm3 in volume (right).

Procedure evaluation

In all patients, either intra-operative (in cystic lesions) or posto-perative radiology evidences (especially in solid lesions) were used for accuracy confirmation. The histopathology results and the operative complications were presented.

Results:

Here we present the co-ordinates of 73 targets in cases previously operated using Egyplan database file and recalculated using Naviplan file to compare target co-ordinates of both.

Table 1 shows the stereotactic shift between the 2 calculations for each target. The stereotactic shifts ranged from 0.02 mm to 1.68 mm with an average vector of 0.47 mm.

Table 1: Comparison between Egyplan and Naviplan co-ordinates to the same target points and the stereotactic distance between them.

Case No	Naviplan (in mm)			Egyplan (in mm)			Distance
	Lat	AP	Ver	Lat	AP	Ver	
1	-36.24	-21.55	30.31	-35.96	-20.17	29.39	1.68
2	-17.39	-11.72	-11.18	-17.44	-12.22	-10.77	0.65
3	-2.1	21.87	11.76	-1.99	21.61	11.84	0.28
4	-4.2	-21.74	8.49	-4.2	-22	8.79	0.4
5	-24.66	54.67	-20.88	-24.6	55.16	-21.92	1.14
6	-31.94	2.69	23.22	-31.98	2.5	23.46	0.3
7	-42.71	4.13	25.5	-42.77	4.04	25.65	0.18
8	-40.42	-0.62	-22.03	-40.44	-0.69	-21.98	0.09
9	-17.44	-11.36	-20.18	-17.43	-11.02	-20.32	0.37
10	-21.71	-11.95	-28.95	-21.7	-12.65	-28.71	0.73
11	8.27	-7.5	-23.87	8.33	-7.9	-23.58	0.49
12	-15.13	-17.63	-15.74	-15.13	-17.58	-15.74	0.05
13	-55.37	1.84	-17.1	-55.49	1.64	-16.94	0.27
14	-29.82	-9.48	-9.9	-29.82	-9.31	-9.93	0.16
15	-16.71	-6.67	-13.34	-16.7	-6.6	-13.38	0.08
16	-10.83	-0.97	4.55	-10.83	-1.12	4.67	0.19
17	-11.81	-7.59	14.49	-11.81	-8	14.68	0.45
18	-44.26	-29.11	-6.03	-44.26	-29.23	-5.94	0.15
19	-18.91	2.06	-41.57	-18.9	2.35	-41.62	0.29
20	-4.9	-1.33	-7.15	-4.9	-1.3	-7.19	0.05
21	-18.4	-27.79	11.36	-18.44	-28.19	11.62	0.48
22	-34.42	-16.45	11.18	-34.42	-16.54	11.44	0.28
23	-27.93	-38.3	-14.42	-27.92	-38.21	-14.62	0.22
24	42.93	-10.76	-37.49	42.88	-11.22	-36.84	0.79
25	-39.52	-30.05	17.23	-39.52	-30.07	16.99	0.24
26	-6.07	-14.25	-12.49	-6.06	-14.71	-12.27	0.5
27	11.07	36.22	12.73	11.11	35.98	13.29	0.61
28	-9.37	7.75	31.47	-9.36	7.82	31.45	0.07
29	-12.83	9.23	-1.13	-12.92	10.49	-2.16	1.63

30	24.9	-33.35	-9.69	24.96	-33.02	-9.82	0.35
31	-15.05	-18.52	14.39	-15.06	-18.58	14.46	0.09
32	-31.98	-40.83	10.45	-32	-41.39	10.79	0.64
33	-27.42	8.89	-13.82	-27.39	8.78	-13.82	0.11
34	-15.87	-7.1	-8.51	-15.77	-8.69	-7.73	1.77
35	22.65	-10.29	-24.65	22.64	-10.25	-24.7	0.06
36	-16.08	-32.92	31.18	-16.1	-33.49	31.66	0.74
37	-5.03	-14.94	29.61	-5.02	-15.04	29.76	0.17
38	-20.42	-14.67	1.17	-20.46	-14.81	1.33	0.21
39	-27.67	-54.42	12.06	-27.64	-54.78	12.41	0.49
40	-15.52	20.49	-19.28	-15.55	20.18	-19.06	0.38
41	-5.15	35.3	-20.49	-5.15	35.23	-20.46	0.06
42	-16.87	16.16	2.39	-16.87	16.2	2.35	0.05
43	-43.28	-56.47	12.63	-43.28	-56.11	12.66	0.36
44	-49	31.57	-11.31	-49	31.43	-11.33	0.13
45	-36.6	-21.81	30.23	-36.63	-20.5	29.73	1.4
46	-2.11	21.97	11.11	-2.1	21.71	11.46	0.44
47	26.21	-28.52	22.36	26.29	-29.28	23.02	1
48	-19	-23.5	-53.87	-19.02	-23.64	-53.81	0.15
49	11.81	-17.91	-11.33	11.79	-17.99	-11.29	0.09
50	26.21	-28.52	22.36	26.29	-29.28	23.02	1
51	11.81	-17.91	-11.33	11.79	-17.99	-11.29	0.09
52	8.16	30.03	12.43	8.16	29.96	12.52	0.12
53	-10.83	-0.97	4.55	-10.83	-1.12	4.67	0.19
54	16.1	-1.23	-11.81	16.1	-1.51	-11.56	0.37
55	-22.16	-31.31	-14.89	-22.16	-31.97	-14.99	0.66
56	2.38	-30.25	25.62	2.38	-29.99	25.64	0.26
57	-34.77	-37.67	12.85	-34.78	-37.79	12.89	0.12
58	-33.72	-16.07	6.82	-33.8	-16.78	7.26	0.83
59	-21.97	-28.19	-2.91	-21.98	-27.56	-2.97	0.62
60	-33.29	-35.15	-6.37	-33.28	-35.48	-6.42	0.33
61	-50.58	-17.5	13.29	-50.69	-17.66	13.48	0.27
62	3.27	1.33	24.55	3.23	1.1	24.83	0.35
63	-23.11	-18.37	4.74	-23.01	-17.97	4.43	0.51
64	-66.27	-25.65	12.12	-66.22	-25.59	12.02	0.12
65	-20.27	23.42	8.63	-20.28	23.32	8.71	0.12
66	-20.26	-26.6	-16.17	-20.23	-27.25	-15.84	0.72
67	-27.82	-7.33	6.2	-27.83	-7.21	6.19	0.12
68	-4.9	-1.33	-7.15	-4.9	-1.3	-7.19	0.05
69	46.12	-18.7	-25.96	46.14	-18.71	-25.96	0.02
70	5.11	4.83	-30.09	5.5	6.41	-31.68	2.27
71	8.1	-14.33	47.06	7.81	-12.25	46.08	2.31
72	22.65	-10.29	-24.65	22.64	-10.25	-24.7	0.06
73	-27.53	9.01	-7.75	-27.51	8.77	-7.59	0.29
Mean							**0.47**

Thirty one patients (13 males and 18 females) with different intracranial lesions were subjected to this method. Table 2 shows sex,

age, lesion characteristics and presentation of them. 42% were males and 58% were females. The patients' age ranged from 1 to 71 years with a mean of 34 years. 48.4% of the lesions were cystic and 51.6% were solid. The lesions were on the right side in 29%, on the left side in 32.2% and midline in 38.7% of cases. The most common presentation was contralateral weakness in 13 cases (41.9%) and manifestations of raised intracranial pressure (hydrocephalus in 6 cases and others in 7 cases) in 13 cases (41.9%), followed by, fits in 4 cases (12.9%), and behavioral changes in 1 case (3.2%). The most common site was the thalamus (26.7%) followed by the suprasellar region (19.4%).

Table 2: Sex, age, lesion characteristics and presentation in the 31 cases included in the study.

Case No	Sex	Age in Years	Lesion			Presentation
			Consist	Side	Site	
1	Male	60	Solid	Rt	Parietal	Fits
2	Female	11	Cystic	Rt	Thalamic	Lt HPR*
3	Female	8	Cystic	Rt	Thalamic	Lt HPR
4	Male	37	Cystic	Lt	Trigonal	Headache
5	Female	1	Cystic	Midline	Suprasellar	HCP**
6	Female	28	Solid	Lt	Thalamic	Rt HPR
7	Female	22	Cystic	Midline	Suprasellar	Visual dist
8	Female	14	Solid	Rt	Thalamic	Lt HPR
9	Male	58	Solid	Rt	Parietal	Lt HPR
10	Female	16	Cystic	Midline	Suprasellar	HCP
11	Male	27	Cystic	Lt	Frontal	Fits
12	Female	26	Solid	Rt	Parietal	Lt HPR
13	Male	55	Solid	Midline	Suprapineal	Behavioral
14	Female	57	Solid	Midline	Suprapineal	Visual dist
15	Female	60	Cystic	Rt	Insular	Lt HPR
16	Female	25	Solid	Lt	Caudate	Headache
17	Female	46	Solid	Lt	Frontal	Rt HPR
18	Male	26	Cystic	Lt	Frontal	Rt HPR
19	Male	12	Cystic	Midline	Suprasellar	Visual dist
20	Male	62	Solid	Lt	Insular	Fits
21	Male	71	Solid	Lt	Trigonal	Visual dist
22	Female	9	Cystic	Midline	Suprasellar	HCP
23	Male	50	Solid	Lt	Thalamic	Rt HPR
24	Female	49	Solid	Lt	Thalamic	Rt HPR
25	Female	33	Solid	Rt	Thalamic	Lt HPR
26	Female	42	Solid	Medline	Pineal	HCP
27	Male	28	Solid	Midline	Genu	HCP
28	Male	10	Cystic	Midline	Brain Stem	HCP
29	Female	62	Cystic	Midline	Frontal	fits
30	Female	35	Cystic	Rt	Thalamic	Lt HPR
31	Male	14	Cystic	Midline	Suprasellar	Visual dist
Mean	**M12/ F18**	**34 Y**	**C15/S16**			

* HPR: Hemiparesis. ** HCP: Hydrochephalus

Table 3 shows the radiological distances between the 3 points refereeing to the spheres' centers as well as the manually derived stereotactic distances and the deference in calculations. The differences ranged from 0.06 mm to 10.17 mm. Of notice is that the mean deference is the least between the pre-auricular spheres (1.78 mm) than the others although the mean distance between these spheres' centers was the longest compared to the others.

Table 3: Radiological and manually derived stereotactic distances between the 3 spheres' centers.

Case No	P1 to P2 Distance in mm			P1 to P3 Distance in mm			P2 to P3 Distance in mm		
	Radio	Stereo	Def	Radio	Stereo	Def	Radio	Stereo	Def
1	151.42	147.29	4.13	107.51	111.57	4.06	114.72	113.58	1.14
2	127.42	132.47	5.05	101.63	107.84	6.21	102.33	108.54	6.21
3	127.5	130.06	2.56	100.03	101.51	1.48	100.2	102.21	2.01
4	138.24	138.65	0.41	110.12	111.34	1.22	113.18	118.52	5.34
5	126.39	130.18	3.79	98.14	97.91	0.23	103.64	104.56	0.92
6	134.18	137.07	2.89	113.06	118.46	5.4	112.94	119.66	6.72
7	133.46	136.14	2.68	104.8	109.18	4.38	106.83	115.27	8.44
8	139.26	140.1	0.84	112.11	117.46	5.35	110.88	116.12	5.24
9	155.3	158.67	3.37	131.89	140.39	8.5	122.71	132.88	10.17
10	135.81	137.29	1.48	105.71	106.64	0.93	94.38	97.24	2.86
11	146.63	148.32	1.69	100.35	98.53	1.82	106.36	105.99	0.37
12	134.89	135.25	0.36	98.09	101.28	3.19	105.46	108.49	3.03
13	132.55	134.71	2.16	99.34	103.79	4.45	100.9	105.28	4.38
14	142.54	145.58	3.04	104.39	109.45	5.06	98.51	105.74	7.23
15	129.29	132.4	3.11	101.67	106.92	5.25	99.79	109.24	9.45
16	130.9	131.81	0.91	106.21	111.31	5.1	100.77	104.29	3.52
17	141.69	145.49	3.8	105.62	113.09	7.47	108.38	114.64	6.26
18	154.04	158.09	4.05	123.51	133.24	9.73	128.4	137.93	9.53
19	129.87	133.13	3.26	108.85	117.9	9.05	104.59	108.8	4.21
20	146.23	148.17	1.94	123.82	133.42	9.6	130.98	140.07	9.09
21	148.63	142.31	6.32	128.08	131.15	3.07	130.47	131.58	1.11
22	121.56	125.39	3.83	110.78	118.14	7.36	100.27	105.91	5.64
23	138.59	142.78	4.19	118.32	122.93	4.61	120.6	126.25	5.65
24	142.73	143.5	0.77	115.53	115.94	0.41	117.31	122.08	4.77
25	133.15	134.97	1.82	115.98	119.24	3.26	113	116.5	3.5
26	141.77	143.45	1.68	117.05	121.18	4.13	110.69	114.16	3.47
27	146.76	147.74	0.98	122.26	123.15	0.89	122.39	123.35	0.96
28	133.63	132.8	0.83	113.69	113.48	0.21	114.27	116.43	2.16
29	128.28	130.78	2.5	109.79	115.13	5.34	106.12	113.7	7.58
30	130.29	130.35	0.06	112.44	113.08	0.64	104.7	109.84	5.14
31	154.75	158	3.25	120.99	124.69	3.7	114.18	119.57	5.39
Mean	137.99	139.77	1.78	111.02	115.14	4.12	110.32	115.11	4.79

The diagnostic yield is the percentage of biopsies with a definitive histopathological diagnosis [9]. In this study the diagnostic yield was 100% for all cases. Table 4 shows the site and histopathology results of the solid lesions studied. The most common site of lesions was in the thalamus. The histopathology results revealed that in descending order of frequency the solid lesions were astrocytoma grade II in 8

cases, glioblastoma multiform in 5 cases. Astrocytoma grade I and grade III and pineal tumor grade I each were found in 1 case.

Table 4: Solid lesions included in the study.

Case No	Site	Histopathology
1	Rt Parietal	AST* WHO G III
6	Lt Thalamic	AST WHO G II
8	Rt Thalamic	AST WHO G II
9	Rt Parietal	AST WHO G II
12	Rt Parietal	GBM WHO G IV
13	Suprapineal	AST WHO G II
14	Suprapineal	AST WHO G II
16	Lt Caudate	GBM WHO G IV
17	Lt Frontal	GBM WHO G IV
20	Lt Insular	AST WHO G II
21	Lt Trigonal	GBM WHO G IV
23	Lt Thalamic	AST WHO G II
24	Lt Thalamic	GBM WHO G IV
25	Rt Thalamic	AST WHO G II
26	Pineal	Pineal tumor Grade II
27	Genu	AST WHO G I

*AST : Astrocytoma.

Table 5 shows the volume, consistency and histopathology results of the cystic lesions studied. In 5 cases the aspirated volume was larger than the estimated volume and in 6 cases less than the estimated volume while it was the same volume in 4 cases.

Table 5: Cystic lesions included in the study.

Case No	Procedure	Lesion			
		Volume (ml)		Color	Histopathology
		Estimated	Aspirated		
2	Aspiration	4	4	Pus	Brain Abscess
3	Aspiration	12	15	Xanthochromic	AST WHO G II
4	Aspiration	40	35	Xanthochromic	AST WHO G III
5	Omya Res	250	100	Engine Oil	CPG*
7	Omya Res	15	12	Oily	CPG
10	Omya Res	18	10	Engine Oil	CPG
11	Aspiration	4	6	Pus	Brain Abscess
15	Aspiration	8	10	Xanthochromic	GBM** WHO G IV
18	Aspiration	12	15	Pus	Brain Abscess
19	Omya Res	50	90	Oily	CPG
22	Omya Res	25	25	Engine Oil	CPG
28	Aspiration	12	10	Xanthochromic	AST WHO G I
29	Aspiration	2	2	Xanthochromic	AST WHO G III
30	Aspiration	2	2	Pus	Brain Abscess
31	Omya Res	42	25	Engine Oil	CPG
Mean	**Mean**	**33**.1	**24.1**		

* CPG: Craniopharyngioma, ** GBM : Glioblastoma Multiform

The histopathology results revealed that in descending order of frequency the cystic lesions were craniopharyngioma (6 cases), astrocytoma (5 cases) and brain abscess (4 cases).

Table 6 shows the histopathology results of all the studied cases. The most common lesion was astrocytoma grade II in 9 cases (29%) followed by glioblastoma multiform in 6 cases and craniopharyngioma in 6 cases (19.4% for each). Others were brain abscess in 4 cases (12.9%), astrocytoma grade III in 3 cases (9.7%), astrocytoma grade I in 2 case (6.5%) and pineal tumor grade II in 1 case (3.2%).

Table 6: Summary of histopathology results in the 31 cases.

Pathology	cases
Astrocytoma Grade I	2
Astrocytoma Grade II	9
Astrocytoma Grade III	3
Glioblastoma Multiform	6
Craniopharyngioma	6
Pineal tumor Grade I	1
Brain Abscess	4
Total	**31**

In one patient (case No 4) there was slight intra-operative bleeding which extended in the Lt lateral ventricle and it was not related to targeting errors as shown by the postoperative CT brain and the histopathology results. The patient was confused and improved gradually without any new deficit. No other neurological complications were found in this series.

Discussion:

We will discuss the accuracy, the safety and the applicability of this new pinless frame-based stereotactic procedure.

- **The accuracy**

The following aspects can affect the procedure accuracy:

First, Naviplan file calculation accuracy:

Quiñones-Hinojosa et al in 2006, found that for the frame-based CRW (which is considered accurate for use in functional stereotaxy) the mean error from the actual target was 1.03 +/- 0.19 mm and the mean target localization error vector was 2.23 +/- 0.14 mm [5].

In a study of 41 targets, the stereotactic shifts between Stereocalc software and Egyplan derived co-ordinates ranged from 0.22 mm to 1.41 mm. The average vector of shift was 0.59 mm [4].

In this study of 73 targets the stereotactic shifts between Naviplan and Egyplan derived co-ordinates, as shown in table 1, ranged from 0.02

mm to 1.68 mm with an average vector of 0.47 mm. It can be assumed that these shifts are practically acceptable.
For more safety, we attached test target to evaluate the accuracy of Naviplan. In the first 3 patients, we used test targets attached to the patient scalp to insure the accuracy of calculations by targeting them before the intended intracranial targets.
The diagnostic yield of stereotaxy ranges between 80 and 99% [7-9]. In this study, 100% diagnostic yield of the histopathology results proves the Naviplan calculation accuracy.
Second, stability of the scalp spherical marks:
The scalp marks were chosen as tunneled radio-opaque spheres with constant radius (3 mm) as shown in figure 1. Their centers are readily detectable in the CT images with the help of these tunnels as shown in figure 2.
To minimize the possibility of displacement in relation to the skull, they were attached over the scalp and two of them were fixed just anterior to the auricles where the scalp is least liable to glide over the skull and the 3rd sphere was attached midline above the glabella. During CT scanning the patient is instructed to avoid moving the head or forehead skin and hence the anterior mark in relation to the skull to stay similar to its position during intraoperative registration. All the sphere sites were marked on the scalp with a pen marker to detect any significant displacement during the procedure.
We calculated the distances between mark centers depending on radiological data and again using manually derived stereotactic data and compared these distances to detect any significant displacement during the procedure. As shown in table 3, the mean deference was the shortest for (point 1 to point 2) distances (1.78 mm) ranging from 0.06 mm to 6.32 mm although the mean distance between these points was the longest both radiologically (137.99 mm) and stereotactically (139.77 mm) compared to the other distances. This can be explained by the fact that the scalp is more firmly adherent to the skull arround the auricles making sphere displacement less liable.
Third, registration of the spherical marks to the frame:
In my opinion, this step is the weakest point in this procedure. This is because I use part of the Radionics arc (figure 5) to manually register spherical marks to the frame cartesian co-ordinate system. Even slight intrapersonal variations are inevitable and affect the resulting target co-ordinates as shown in table 3. One can suggest using the whole Radionics arc for more accurate registration but this way will be time consuming and increases the liability of head movement during the procedure leading to less accurate results. The mean differences shown in table 3 are attributed mainly to the errors of manual stereotactic registration although slight displacements of the spheres

may have a role. Based on these depicted differences, we recommend that the targets should be at least 2 ml in volume to be approached by the current method to overcome these problems till better registration method is applied.

- **The safety**

Movement of the head after registration of the spheres can occur. In one procedure, one patient moved his head just after registration of the spheres because of anesthesia wear off and forced us to repeat the registration step after anesthesia control. This shows the importance of deep anesthesia in the procedure. It is of atmost importance that the head doesn't move while the biopsy needle is inside the brain because the brain will move against a fixed needle which can cause catastrophic brain injury. Every effort should be done to avoid this problem.

We repeated surgical field sterilization before and after registration to guard against infection. In fact there was no surgery related infection in this series.

In one patient (case No 4) there was slight intra-operative bleeding which extended in the Lt lateral ventricle and it was not related to calculation errors.

- **The applicability**

We present 4 examples where stereotaxy using pin fixation was not applicable and the new pinless method was used:

In the first example (Case No 2, 11 years old female having a small right thalamic cystic lesion) the frame fixation failed after the initial steps of a classic frame based stereotactic procedure were done including CT brain scanning because of her small sized head. Her radiologically estimated lesion volume was about 4 ml and we decided to do the operation with this new pinless method.

In the second example (Case No 5, 1 year old female with suprasellar cystic lesion) the skull was not rigid enough to hold the pins so pin fixation was not suitable. We decided to insert Omya reservoir using this pinless method.

In the third example (Case No 6, 28 years old female with left thalamic intra-axial mass) the trial of pin fixation was accompanied with sever attacks of vomiting that forced us to cancel the operation and her vomiting lasted for more than 12 hours and, in the next surgical list, we decided to do the operation with the pinless technique.

In the fourth example (Case No 31, 14 years male with a recurrent suprasellar cystic lesion) a previous frontal craniectomy defect made pin fixation for stereotaxy unsuitable. We inserted Omya reservoir for him using this pinless technique.

Advantages of the pinless method over pin fixation:

1. It avoids painful pin fixation and its hazards including penetration injuries and intubation difficulties.
2. It can be applied in infants with soft skulls.
3. It can be applied in patients with small skulls and in those patients with cranial defects who can't hold stereotactic pins.
4. It can be easily relocated when needed. For example when a cyst recollects at the same site.

Restrictions of the current method:

1. When the target is near to the cranial vault, it is important to choose a suitable entry point either with a CT mark during the same procedure or during the operation in a special step. If the entry point is away from the target that is near the cranial vault, the trajectory may not be suitable.
2. I recommend that the targets should not be less than 2 ml in volume to overcome registration errors by the current method. Better registration can help to accurately approach smaller targets.
3. The position of the sphere marks link may restrict the burr hole site but the marks can be fixed to the scalp with a glue to avoid this when needed. In this series we didn't need such burr holes.
4. The current method is not suitable for functional targets until better registration method is available making it comparable to frameless stereotaxy.

Conclusion: Frame-based pinless stereotaxy with Naviplan is save, accurate and easier for the patients, and can be useful in situations where rigid pins can't be applied.

Reference:

1. **Michael Schulder:** Stereotactic Surgery with the Radionics Frame. Handbook of Stereotactic and Functional Neurosurgery. by Marcel Dekker, Inc, p 46; 2003.
2. **Reavey-Cantwell JF, Bova FJ and Pincus DW:** Frameless, pinless stereotactic neurosurgery in children. J Neurosurg. Jun;104(6 Suppl):392-5; 2006.
3. **Devin V Amin, MD, Karl Lozanne, MD, Phillip V Parry, MD, Johnathan A Engh, MD, Kathleen Seelman, PA-C, and Arlan Mintz, MD**: Image-guided frameless stereotactic needle biopsy in awake patients without the use of rigid head fixation. J Neurosurg 114:1414–1420, 2011.
4. **Abdin K Kasim:** Frame-Based Stereotaxy Using Egyplan File for Voxel-Based Target Calculation. Scientific Journal of Sohag Faculty of Medicine, , Jan 2013 Vol 17, No 1, pp 19-23.

5. **Quiñones-Hinojosa A, Ware ML, Sanai N and McDermott MW:** Assessment of image guided accuracy in a skull model: comparison of frameless Stereotaxy techniques vs. frame-based localization. J Neurooncol. Jan;76(1):65-70, 2006.

6. **Yi Lu, MD PhD*, Cecil Yeung, Alireza Radmanesh, MD, Robert Wiemann, Peter M. Black, MD PhD, and Alexandra J. Golby, MD:** Comparative Effectiveness of Frame-based, Frameless and Intraoperative MRI Guided Brain Biopsy Techniques. World Neurosurg. 2015 March ; 83(3): 261–268. doi:10.1016/j.wneu.2014.07.043.

7. **Fritsch MJ, Leber MJ, Gossett L, Lulu BA, Hamilton AJ:** Stereotactic biopsy of intracranial brain lesions. High diagnostic yield without increased complications: 65 consecutive biopsies with early postoperative CT scans. Stereotact Funct Neurosurg 1998; 71: 36–42.

8. **Yu X, Liu Z, Tian Z et al:** Stereotactic biopsy for intracranial space-occupying lesions: clinical analysis of 550 cases. Stereotact Funct Neurosurg 2000; 75: 103–108.

9. **Fügen V. Aker, Tayfun Hakan, Selhan Karadereler and Murat Erkan:** Accuracy and diagnostic yield of stereotactic biopsy in the diagnosis of brain masses: Comparison of results of biopsy and resected surgical specimens. Neuropathology 2005; 25, 207–213.

ملخص البحث

عنوان البحث:

جراحة المخ المجسمة المستندة إلى إطار بدون مسامير.

الباحث:

دكتور / عابدين خيرالله قاسم – مدرس جراحة المخ والأعصاب بكلية الطب – جامعة سوهاج

مقدمة:

تهدف جراحة المخ المجسمة المستندة إلى الإطار إلى الوصول إلى الآفات الدماغية بدقة من خلال تثبيت إطار إلى الجمجمة بمسامير وإحالة الأهداف الدماغية إلى هذا الإطار تليها جراحة موجهة به. ويعد تثبيت المسامير هو الخطوة المؤلمة في العملية وفي بعض الحالات قد يكون من الصعب القيام به كما في الأطفال الصغار ذوي الجماجم المرنة أو الصغيرة أوفي المرضى الذين يعانون من عيوب غير مناسبة بالجمجمة أو تربنة سابقة. من ناحية أخرى، لا يوجد جهاز جراحة المخ المجسمة في العديد من المراكز.

الهدف:

لتقييم تقنيتنا الجديدة في جراحة المخ المجسمة المستندة إلى إطار بدون مسامير باستخدام برنامج قاعدة بيانات مصممة شخصيا، نافيبلان.

الأساليب:

نثبت ثلاث علامات كروية صغيرة يمكن رؤيتها بالأشعة المقطعية إلى الجمجمة ويتم إحالة الهدف الدماغي إلى نظام الإحداثيات الديكارتية على أساسها. ثم يتم تسجيل العلامات إلى الإطار ويتم نقل مراجع الهدف من نظام الإحداثيات الديكارتية على أساس هذة العلامات إلى نظام الإحداثيات الكارتيزي المبني على الإطار باستخدام ملف قاعدة بيانات مصممة شخصيا (نافيبلان).

النتائج:

تعرض ٣١ مريضا لهذه الطريقة ، واستخدمت في جميع المرضى إما أدلة أثناء الجراحة أو الأشعة بعد الجراحة للتأكد من دقة الإستهداف. وفي ١٥ حالة أكد تفريغ الآفات الدماغية السائلة والاشعة المقطعية بعد العملية الجراحية دقة الإجراء. ، بينما أظهرت الاشعة المقطعية بعد العملية الجراحية وكذلك فحص الأنسجة المستخرجة في ١٦ حالة من الآفات الدماغية الصلبة أنها استهدفت بدقة مقبولة.

الاستنتاج:

جراحة المخ المجسمة المستندة إلى الإطار بدون مسامير باستخدام ملف نافيبلان سهلة وآمنة ودقيقة ويمكن أن تكون مفيدة خاصة في الحالات التي لا يمكن تثبيت المسامير فيها.

الكلمات الإفتتاحية:

جراحة المخ المجسمة بدون مسامير ، الاستهداف ثلاثي الأبعاد ،آفات الدماغ العميقة، الجراحة المجسمة.